Journal of Basic and Environmental Sciences

ISSN
Online:2356-6388
Print:2536-9202

Research Paper Open Access

Synthesis and characterization of zinc oxide nanoparticles using hydrothermal method

M. M. Abdel Fattah, A. A. Ali and I. S. Ahmed

Chemistry Department, Faculty of Science, Benha University, Benha, Egypt

Corresponding author: email: marwa.mohamed199900@gmail.com, Tet: +201090610969

Abstract

Zinc oxide nanoparticles were synthesized by hydrothermal method using zinc acetate dihydrate as a metal precursor and NaOH at pH 9 using different temperatures: 100^{o}C, 120^{o}C and 135^{o}C for 1 hour, separately. The synthesized zinc oxide nanoparticles were characterized by X-ray diffraction (XRD), UV-Visible spectroscopy (UV-Vis), Fourier Transform Infrared spectroscopy (FT-IR) and diffuse reflectance spectroscopy. Crystal sizes, band gap and color axes of the synthesized nanoparticles samples were determined using XRD and DRS spectroscopy.

Keywords: Zinc oxide nanoparticles, hydrothermal method, XRD, FT-IR.

1. Introduction

Nanomaterials, with their special qualities, are considered one of the most promising new materials of the twenty-first century and play an indispensable role in many fields. Because of their minuscule sizes and sharply increased specific surface area, nano-zinc oxides exhibit unique characteristics in the areas of magnetic, optical, electrical, chemical, and catalytic aspects. Thus, the nano-zinc oxides have been applied as a novel kind of inorganic material with multiple uses [1]. With a large bandgap and a high exciton binding energy, zinc oxide is a transition metal oxide semiconductor.

ZnO is therefore one of the most favored materials in the field of optoelectronic research [2]. It is an inexpensive substance that is widely found

in nature[3]. ZnO nanoparticle morphology is easily modifiable[4]. ZnO nanostructures have high electron mobility [5].

Various synthesis methods have been developed and classified into three main groups: chemical, biogenic, and physical (green method). Electrodeposition, magnetron sputtering, pulsed laser deposition, and electron beam evaporation are examples of physical procedures[6-10]. The path of chemical synthesis includes the following methods: spray pyrolysis, microemulsion, hydrothermal, solvothermal, sol-gel, chemical bath deposition, wet chemical process, precipitation and combustion[11-19]. The biogenic synthesis of metal oxide nanoparticles is mediated by microbes or plants, and the resulting extracts are biocompatible and can act as stabilizing agents for the NPs. The environment is poisoned by chemical synthesis, but pure, desirable crystals with great stability and yield are generated [20]. Numerous researchers have been drawn to the hydrothermal approach due to its many benefits, which include low cost, easy preparation, and minimal equipment requirements [21]. The primary determinants of nanoparticle morphology are temperature, reacting solution concentration, and reaction time. This in turn has an effect the physical and chemical properties of nanoparticles [2].

In this work, zinc oxide is prepared using hydrothermal method at different method (100°C, 120°C, 135°C) separately. pH of solution mixture is kept as 9. Several instruments are used to characterize the produced zinc oxide nanoparticles.

2. Experimental details

2.1. Materials and reagents

Zinc acetate hexahydrate $Zn(CH_3COO)_2.6\ H_2O$ (purity 98%). sodium hydroxide NaOH sheets (purity 98%) from Al-Nasr Chemicals Company. During the experiment, distilled water was utilized.

2.2. Synthesis

20 mM Zinc acetate was dissolved in 30ml distilled water under stirring for 30 min. After completely soluble then 3 M NaOH was added drop by drop to reach pH 9. Drop by drop, the NaOH solution is added to the old gel while being constantly stirred. This solution mixture was transferred into Teflon lined sealed stainless-steel autoclaves and kept in hydrothermal oven at a temperature of 100 °C for 1 h. The beaker was then allowed to cool naturally to room temperature outside. After filtering, the resulting solution was rinsed with distilled water

and allowed to dry at 70°C. The experimental procedure is repeated for 120 °C and 135 °C by keeping 1 hour fixed, and samples were named as Z1, Z2 and Z3 respectively.

2.3. Characterization

Crystal structure and average crystallite size were measured by XRD Rigaku Mini Flex 600 diffractometer. purity of samples was confirmed by FT-IR model BRUKER ALPHA II at from 4000 to 400 cm^{-1}. UV-Visible absorption is measured by (Jasco; model V 670) spectrophotometer.

3. Results and discussion

3.1. XRD study

Figure (1) showed XRD patterns of the ZnO nanoparticles prepared by hydrothermal method in the range of 10–70°. The synthesized zinc oxide (Z1, Z2 and Z3) appeared the pure phase of zinc oxide according to card no (1011258, 2107059), (8) and (2300112) respectively.

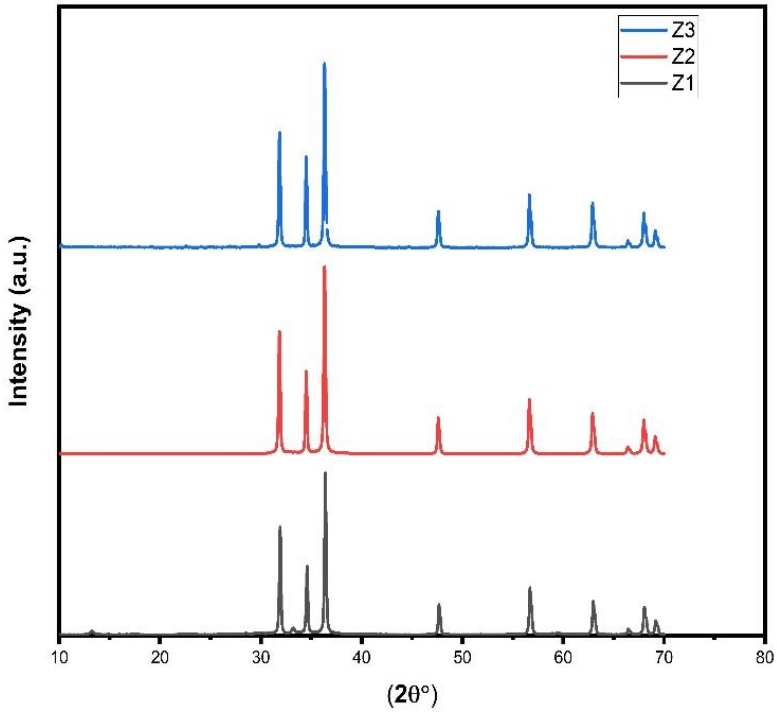

Figure (1): XRD patterns of the synthesized zinc oxide at different temperatures (Z1, Z2 and Z3 samples) using hydrothermal method.

the average crystalline size of these nanoparticles was determined by the Debye Scherrer equation as shown in equation (1)

$$D = k\lambda/B\cos\theta, \quad (1)$$

where B is the full-width half maximum, k is the Scherrer constant, D is the crystallite size, and λ is the wavelength of X-ray. XRD shows that the average sizes are 32 nm, 52 nm and 57 nm for Z1, Z2 and Z3 respectively.

3.2 FTIR

(FT-IR) of the prepared zinc oxide (Z1, Z2 and Z3 samples) was in the range of 400-4000 cm^{-1} shown in figure (2). peaks at 420-450 cm^{-1} related to the vibration of Zn-O in zno lattice. The bending and stretching vibration modes of the adsorbed water on the surface of the produced zinc oxide nanoparticles are represented by the absorption peaks at 1610-1615 cm^{-1} and 3400-3450 cm^{-1}[22].

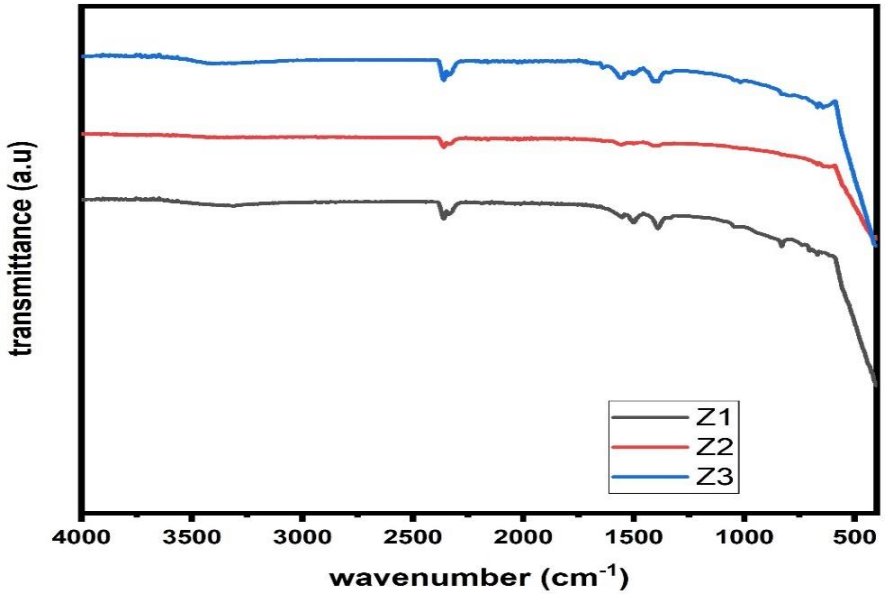

Figure (2): FT-IR patterns of the synthesized zinc oxide at different temperatures (Z1, Z2 and Z3 samples)

3.3 Optical Studies

UV absorption spectra of the obtained zinc oxide (Z1, Z2 and Z3) between 200 and 800 nm are examined. Figure 3 displays the UV–Vis and NIR diffuse reflectance spectra of the samples. The Z1, Z2, and Z3 samples exhibit the reflectance edge at 369 nm, 371 nm, and 372 nm, respectively. The diffuse reflectance data is regenerated into equivalent absorption coefficients (α) using the Kubelka–Munk function, as shown in Fig. 4. The Kubelka Munk function can be found using Equation (2)

$$\boldsymbol{F(RE) = (1 - RE)^2/2RE} \qquad \textbf{(2)}$$

RE: the reflectance data of the sample. F(RE): Kubelka Munk function.

The absorption band for Z1, Z2, and Z3 is located at 366 nm, 370 nm, and 361 nm, respectively, in the zinc oxide spectrum.

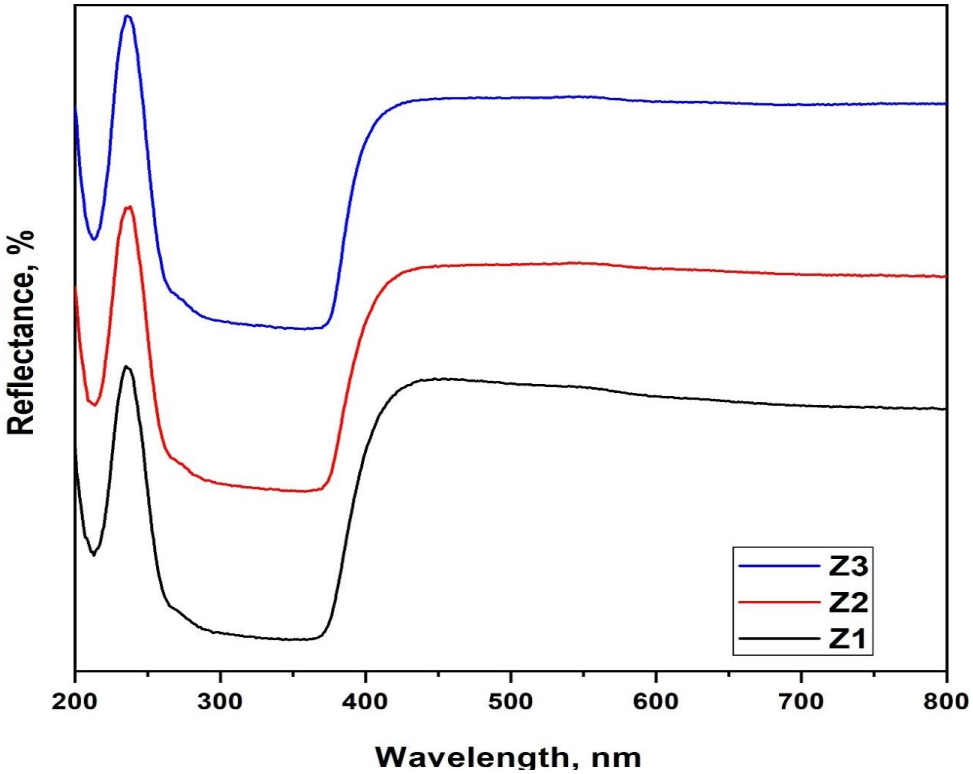

Figure (3): UV–Vis diffuse reflectance spectra of the synthesized zinc oxide at different temperatures (Z1, Z2 and Z3 samples).

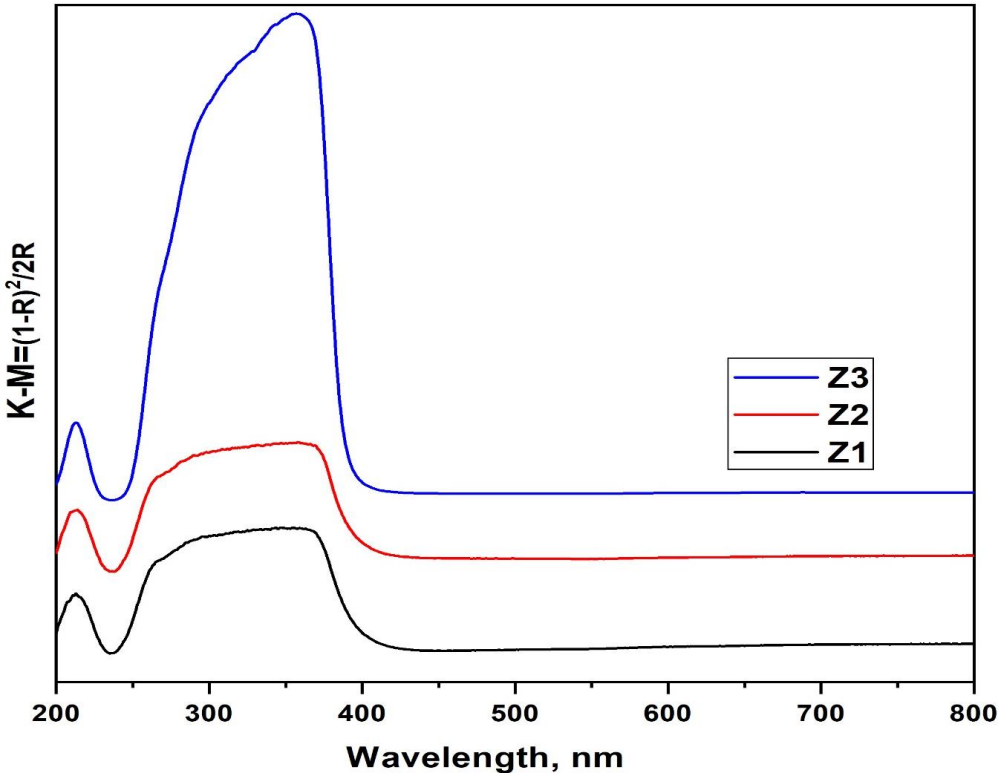

Figure (4): UV-VIS and NIR absorption spectra of synthesized zinc oxide at different temperatures (Z1, Z2 and Z3 samples).

The Eq. can be used to calculate the prepared powder's direct and indirect band gaps.

$$(F(RE)h\upsilon) = D(h\upsilon - Eg)^{n}$$

The energy function is F(*h*υ). the reflectance of the samples is R. D is constant and the value of n, which depends on the permitted direct and indirect electronic transitions, ranges from 1/2 to 2.

As seen in Fig 5, the direct and indirect band gaps are calculated utilizing the relationship between $(F(RE)h\upsilon)^{1/n}$and (hυ).

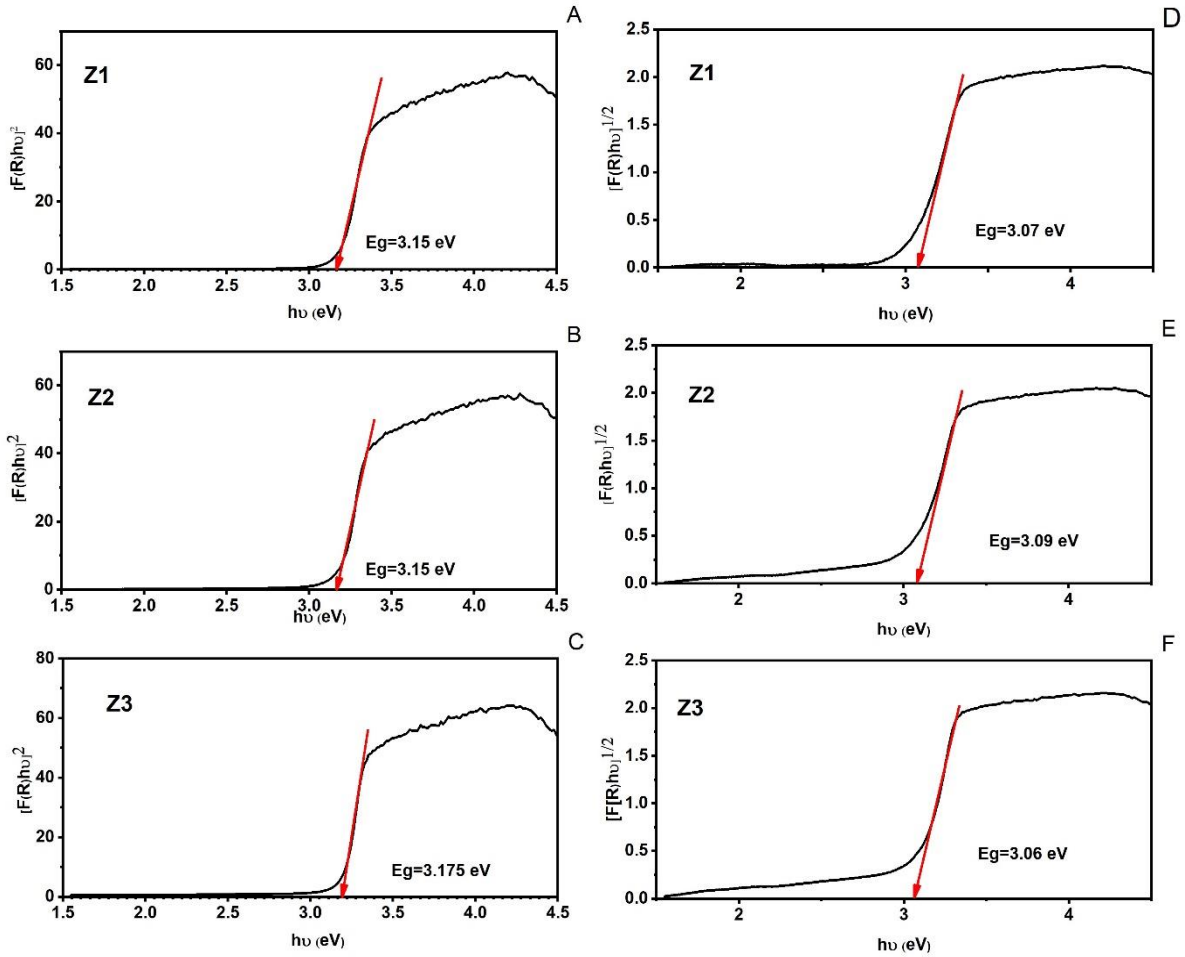

Figure (5): direct band gap calculation (**a**–**c**) and indirect band gap calculation (**d**–**f**) of the synthesized zinc oxide (Z1, Z2 and Z3 samples).

In accordance with the CIE-lab and CIE-LCH analysis procedures, color parameters were determined using colorimetric techniques. (91.85/-1.57 /0.27 / 1.59/ 170.41), (91.97/-1.29 /-1.47 / 1.96/ 228.82), and (95.14/-1.56/ -1.17/ 1.95/ 216.93) were the L/a/b/c/H values for Z1, Z2, and Z3, respectively. The parameters showed the high lightness of all samples.

IISK5602: 2008 and JISA5759: 2008 techniques were used to determine the synthesized sample's light and solar reflectance. According to JISA5759: 2008, the light and solar reflectance values for Z1, Z2, and Z3 were (87.95 % / 76.16 %) , (80.36 % / 67.66 %) , and (80.64 % / 68.36 %) respectively. Moreover, the solar reflectance for Z1, Z2, and Z3 was found to be (81.82 % / 67.43 % / 75.43 %), (74.64 % / 56.82 % / 66.73 %), and (75.47 % / 57.17 % / 67.36 %) using the IISK5602: 2008 technique. The extracted data showed that the synthesized samples have high light and sun reflectance.

4. Conclusion:

Zinc oxide synthesized by hydrothermal method under different reaction temperatures (100^{o}C, 120^{o}C and 135^{o}C). The obtained zinc oxide nanoparticles (Z1, Z2, and Z3 samples) have been studied using a variety of techniques, including FT-IR, DRS, and XRD. The crystal of nanoparticles is determined to be 32 nm, 52 nm and 57 nm for Z1, Z2 and Z3 respectively. The structural characteristics of nanomaterials were shown changed in response to a change in reaction temperature by XRD analysis. The direct band gaps are determined to be 3.15, 3.175, and 3.15 eV, respectively. The indirect band gaps are determined to be 3.07, 3.09 and 3.06 eV, respectively. According to colorimetric techniques, the synthesized samples have high lightness. The synthesized samples of zinc oxide have high light and sun reflectance.

Acknowledgement

The authors thank the Academy of Scientific Research for funding the research within the Next Generation Scientists Scholarship. The authors express thanks to Chemistry Department, Faculty of Science, Benha University, Egypt for support the research.

Code # BUFS-REC-2023-59Chm

5. References

1. Liu, W., et al., *Supercritical hydrothermal synthesis of nano-zinc oxide: Process and mechanism.* Ceramics International2022. **48**(16): p. 22629-22646.
2. Mohan, S., et al., Hydrothermal synthesis and characterization of Zinc Oxide nanoparticles of various shapes under different reaction conditions. Nano Express, 2020. 1(3): p. 030028.
3. Naveed Ul Haq, A., et al., Synthesis approaches of zinc oxide nanoparticles: the dilemma of ecotoxicity. Journal of Nanomaterials, 2017. 2017(1): p. 8510342.

4.Chu, H.O., et al., *Structural, optical properties and optical modelling of hydrothermal chemical growth derived ZnO nanowires.* Transactions of Nonferrous Metals Society of China 2020. **30**(1): p. 191-199.

5. Hassanpour, M., H. Safardoust-Hojaghan, and M.J. Salavati-Niasari, *Rapid and eco-friendly synthesis of NiO/ZnO nanocomposite and its application in decolorization of dye.* Journal of materials science: materials in electronics, 2017. **28**: p. 10830-10837.

6. Chhikara, D., M.S. Kumar, and K. Srivatsa, *On the synthesis of Zn/ZnO core–shell solid microspheres on quartz substrate by thermal evaporation technique.* Superlattices Microstructures, 2015. **82**: p. 368-377.

7. Kwoka, M., et al., *Surface properties of nanostructured, porous ZnO thin films prepared by direct current reactive magnetron sputtering.* Materials, 2018. **11**(1): p. 131.

8. Maleki-Ghaleh, H., et al., *Evaluation of the photo-electro-catalytic behavior of nano-structured ZnO films fabricated by electrodeposition process.* Materials Letters, 2016. **169**: p. 140-143.

9. Ren, X., et al., *Fabrication gallium/graphene core–shell Nanoparticles by pulsed laser deposition and their applications in surface enhanced Raman scattering.* Materials Letters, 2015. **143**: p. 194-196.

10. Varnamkhasti, M.G., H.R. Fallah, and M. Zadsar, *Effect of heat treatment on characteristics of nanocrystalline ZnO films by electron beam evaporation.* Vacuum, 2012. **86**(7): p. 871-875.

11. Ahmed, I., H. Dessouki, and A. Ali, *Synthesis and characterization of NixMg1− xAl2O4 nano ceramic pigments via a combustion route.* Polyhedron, 2011. **30**(4): p. 584-591.

12. Ali, A., et al., *Sol-Gel Auto-Combustion Preparation and Characterization of Silica Nanoparticles for The Removal of Congo Red Dye from Aqueous Media.* 2020. **5**(7 part (1)-(2)): p. 199-208.

13. Ali, A.A. and I.S. Ahmed, *Sol-gel auto-combustion fabrication and optical properties of cobalt orthosilicate: Utilization as coloring agent in polymer and ceramic.* Materials Chemistry Physics, 2019. **238**: p. 121888.

14. Ali, A.A., et al., *Auto-combustion fabrication and characterization of TiO2*

nanoparticles and utilization as an adsorbent for removal of Pb2+ from aqueous solution. Desalination Water Treatment, 2020. **193**: p. 83-94.

15. Ali, A.A., S.A. Shama, and S.R. EL-Sayed, *Fabrication, structural and adsorption studies of zirconium oxide nanoparticles.* Benha Journal of Applied Sciences, 2020. **5**(7 part (1)-(2)): p. 245-253.

16. Dwivedi, S., et al., *Reactive oxygen species mediated bacterial biofilm inhibition via zinc oxide nanoparticles and their statistical determination.* PloS one, 2014. **9**(11): p. e111289.
17. E Marghany, N., et al., *Zirconium oxide nanoparticles: Fabrication, study and application for removal of organic dye from aqueous media.* Benha Journal of Applied Sciences, 2022. **7**(5): p. 193-200.

18. Venu Gopal, V. and S. Kamila, *Effect of temperature on the morphology of ZnO nanoparticles: a comparative study.* Applied Nanoscience, 2017. **7**: p. 75-82.

19. Zhu, L., Y. Li, and W. Zeng, *Hydrothermal synthesis of hierarchical flower-like ZnO nanostructure and its enhanced ethanol gas-sensing properties.* Applied Surface Science, 2018. **427**: p. 281-287.

20. Droepenu, E.K., et al., *Zinc oxide nanoparticles synthesis methods and its effect on morphology: A review.* Biointerface Res. Appl. Chem, 2022. **12**: p. 4261-4292.
21. Babu, K.S. and V. Narayanan, *Hydrothermal synthesis of hydrated zinc oxide nanoparticles and its characterization.* Chemical Science Transactions, 2013. **2**(S1): p. S33-S36.

22. Ali, A.A., et al., *Auto-combustion fabrication and optical properties of zinc oxide nanoparticles for degradation of reactive red 195 and methyl orange dyes.* InorganicOrganometallic Polymers Materials 2021. **31**: p. 3780-3792.